ISSN 1674-1056
http://cpb.iphy.ac.cn
http://iopscience.iop.org/cpb
中国物理 B
Chinese Physics
中国物理 Chinese Physics B

Photonic crystal structures: Beam deflector and beam router

Utku Erdiven, Erkan Tetik, Faruk Karadag
Citation: Chin. Phys. B . 2018, 27(4): 044204. **doi:** 10.1088/1674-1056/27/4/044204

Journal homepage: http://cpb.iphy.ac.cn; http://iopscience.iop.org/cpb

What follows is a list of articles you may be interested in

Further analysis of scintillation index for a laser beam propagating through moderate-to-strong non-Kolmogorov turbulence based on generalized effective atmospheric spectral model

Jing Ma(马晶), Yu-Long Fu(付玉龙), Si-Yuan Yu(于思源), Xiao-Long Xie(谢小龙), Li-Ying Tan(谭立英)
Chin. Phys. B . 2018, 27(3): 034201. **doi:** 10.1088/1674-1056/27/3/034201

(3+1)-dimensional localized self-accelerating Airy elegant Ince-Gaussian wave packets and their radiation forces in free space

Dongdong Li(李冬冬), Xi Peng(彭喜), Yulian Peng(彭玉莲), Liping Zhang(张丽萍), Xingyu Chen(陈星宇), Jingli Zhuang(庄经立), Fang Zhao(赵方), Xiangbo Yang(杨湘波), Dongmei Deng(邓冬梅)
Chin. Phys. B . 2017, 26(12): 124202. **doi:** 10.1088/1674-1056/26/12/124202

Orbital angular momentum density and spiral spectra of Lorentz-Gauss vortex beams passing through a single slit

Zhi-Yue Ji(季志跃), Guo-Quan Zhou(周国泉)
Chin. Phys. B . 2017, 26(9): 094202. **doi:** 10.1088/1674-1056/26/9/094202

Laser beam shaping with magnetic fluid-based liquid deformable mirrors

Zhi-Zheng Wu(吴智政), Zhu Zhang(张柱), Xiang-Hui Kong(孔祥会), Jun-Qiu Wu(吴君秋), Tao Wang(王韬), Mei Liu(刘梅), Shao-Rong Xie(谢少荣)
Chin. Phys. B . 2017, 26(7): 074201. **doi:** 10.1088/1674-1056/26/7/074201

Role of the aperture in Z-scan experiments: A parametric study

M. R. Rashidian Vaziri
Chin. Phys. B . 2015, 24(11): 114206. **doi:** 10.1088/1674-1056/24/11/114206

Photonic crystal structures: Beam deflector and beam router

Utku Erdiven[1], Erkan Tetik[2,†], and Faruk Karadag[1]

[1] *Department of Physics, Arts and Sciences, Cukurova University*, 01100, *Adana, Turkey*
[2] *Computer Education and Instructional Technology, Department of Education, Usak University*, 64200, *Usak, Turkey*

(Received 22 October 2017; revised manuscript received 25 December 2017; published online 10 March 2018)

We investigate the optical characteristic, transverse magnetic (TM) and transverse electric (TE) band of two-dimensional (2D) square lattice photonic crystal structure, which is composed of cylindrical air regions positioned at the corners of the square shaped dielectric rods. We obtain the wide photonic bandwidths between TM1–TM2 and TM3–TM4 bands. According to the results, we demonstrate the band gaps close to each other in the TM and TE frequencies for proposed structures. The resulting photonic gaps are formed to be about 8% at the higher frequencies of TE modes (TE4–TE5) and TM modes (TM7–TM8 and TM9–TM10). In addition, we examine isotropically generated structures for light guiding properties and observe that the light is directed in a particular route without using any deflection. We also investigate the self-collimation effect with the designed structure. The obtained results reveal the influences of the radius of cylindrical air holes and the angle between these air holes on absolute and partial photonic band gaps. Moreover, we observe the TM and TE band gaps that overlap. It is thought that the obtained band overlap will provide an easy way to produce the photonic crystals in practical applications like photonic insensitive waveguide. It is also believed that these results can provide the photonic crystal structures to work as a beam deflecting and beam router in integrated optical circuit applications.

Keywords: photonic bandgap materials, electromagnetic wave propagation, beam characteristics

PACS: 42.70.Qs, 41.20.Jb, 29.27.Fh **DOI:** 10.1088/1674-1056/27/4/044204

1. Introduction

Photonic crystals (PCs) which were first proposed in 1987[1] have attracted considerable attention from researchers due to their optical characteristics.[2–4] The permittivity values of PCs changes in one, two, or three dimensions, depending on their geometric structures. In this way, each of the PCs has a large number of lattice types and demonstrates attractive features that can be used in many areas such as waveguides, optical insulators, splitters, and optical devices.[5–7] For example, they are well known for their ability to check and manage the propagation of electromagnetic waves in restricted space. PCs which have photonic frequency band gaps are suitable structures to suppress and direct the incident energy. Due to these unique features of PCs, they are applicable to the integrated photonic circuits,[8–11] polarization insensitive optical devices,[12,13] beam splitters,[14,15] optical compact triplexer,[16] filters,[17] laser,[18] negative refraction,[19–22] polarization-selective splitter,[23] Mach–Zehnder interferometer,[24,25] and multifunctional gradient index (GRIN).[26–28] The photonic band gap (PBG) which occurs within the photonic crystal is regarded as a most significant feature.[29,30] The PBG is represented by the energy or frequency range in which the PC prevents light from propagating. Thus, all the optical modes are prohibited from occurring in PBG. But, optical modes in PCs can be directed or guided to a desired point. This situation is achieved by waveguides and cavities. So, the light can propagate at the frequencies of the PBG. Furthermore, these cases can be formed by breaking the symmetry of the PC structure or by making a change of unit cell size (structural configuration). All these mentioned specific dispersion characteristics are obtained by anisotropic photonic crystals in the absence of structural defects.

Recently, various studies about the anisotropic optical properties of two-dimensional (2D) PCs were carried out.[31–33] An anisotropic structure formed in a periodic medium can be obtained through the dielectric parameter. These structures which may have lower symmetry can show super-prism and self-collimation effects. Thus, there is no need to create wave defects. There are also PC waveguide bend studies showing the self-collimation effect on structure.[34,35] All of these cases distort the light beam from its route and guide it along the desired route. The guidance of electromagnetic wave in a PC is efficiently succeeded by the self-collimation effect. It means that its construction of the dispersion acts as the PC structure like the collimation of incident wave with a specified angular range along the desired directions. Self-collimation provides constricted lateral limitations without physical boundaries and coupling into narrow waveguides without perfect arrangement. Besides, it is possible to guide light over a larger bandwidth with respect to the line defect counterpart. Applications of the self-collimation effect present new challenges to research such as self-guiding,[36,37] spatial beam routing,[38,39] and beam-splitting.[40,41] When the previous studies about PCs are checked, it can be seen that they generally contained symmetric structures. Dielectric rods used in these symmetric structures are mostly in cylindrical

†Corresponding author. E-mail: erkan.tetik@usak.edu.tr

© 2018 Chinese Physical Society and IOP Publishing Ltd

and elliptical shapes. However, PC structures proposed in the present work contain square dielectric rods. We position the cylindrical air holes at the corners of these square dielectric rods. Even though this structure is formed as an isotropic structure, it yields anisotropic optical properties. Our goal is to obtain the absolute photonic bandwidth for TM and TE polarization in the structure, to investigate the influence of self-collimation of the structure and to guide the light through a specific route in PC structure without lattice defects according to the obtained iso-frequency contours. At the same time, for determining the direction and the speed of the electromagnetic wave in PC, the contours of the natural modes are examined. These contours reveal the interaction between the light and the matter. In this regard, many researchers have dealt with it in different ways like the self-collimation effect by looking at the natural mode curves in order to control light propagation.[42,43] In this context, we aim to deliver an additional solution for the parametrical adjustments of ultra-compact integrated devices. We make these adjustments on the symmetry of the photonic crystal structure to achieve wide photonic band spacing. Furthermore, it is believed that this study will create a new application area for GRIN medium, and also our work can provide a new contribution to photonic band gap engineering.

We use the plane wave expansion (PWE) method to compute the absolute PBG and ensure that enough plane waves are used for dispersion analysis of PC. The rest of this paper is organized as follows. In Section 2, we analyze the dispersion properties of the designed PC. In Section 3, we investigate the self-collimation effect and simulation results with iso-frequency contours for proposed PC structures using the finite-difference-time-domain (FDTD) method and PWE method. In Section 4, we demonstrate a different application to the designed photonic crystal Y branch structure.

2. Proposed and designed 2D photonic crystal structures

The 2D square dielectric rods are embedded in the air to create a PC structure as shown in Fig. 1. The sizes of the square dielectric rods are the same ($d = 0.6a$), which is based on silicon with high dielectric constant ($\varepsilon_r = 12$ at 1500 nm). There are cylindrical air gaps, each of which has a radius of $r = 0.20a$, located in the corners of quadratic dielectric rods. The centers of cylindrical gaps are assigned as the corners of the quadratic dielectric rods (O, O_1, O_2, O_3, and O_4). The PC band structure is examined with the plane wave method. The 2D PC is periodically arranged along the x–y direction and assigned to be infinite along the z direction as shown in Fig. 2. Therefore, the absolute PBG is evaluated throughout on the x–y plane. Any mode of optical signals in this absolute PBG cannot be transmitted throughout the PC. However, the harmonic modes are decomposed into two polarizations, i.e., transverse magnetic (TM) mode and transverse electric (TE) mode due to the mirror symmetry.

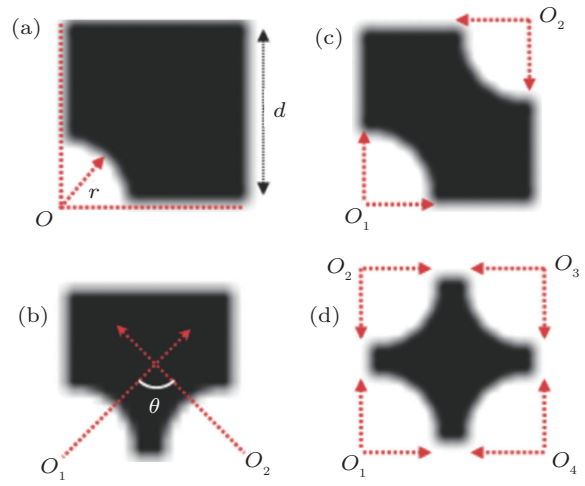


Fig. 1. (color online) Designed PC structures. The generation of the final form of unit cell occurs by moving from panel (a) to panel (b). Centers of the cylindrical air rods are at the corners of square dielectric rods (O, O_1, O_2, O_3, and O_4).

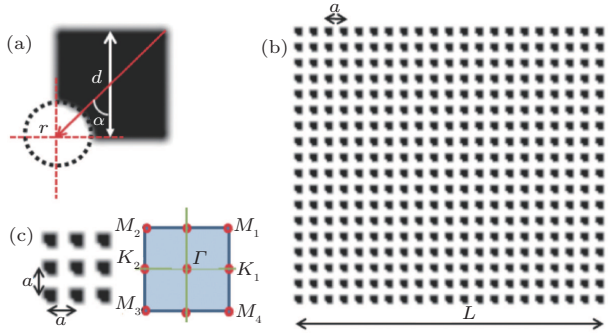


Fig. 2. (color online) (a) Proposed photonic crystal structures. Dielectric constant of square dielectric rod is 12 and radius of cylindrical hole is $0.20a$. Side of dielectric rod is $d = 0.60a$. Here, α angle is $-45°$. (b) Generated finite size square lattice of the designed photonic crystal structure. (c) Brillouin zone of the worked photonic crystal structure. $\Gamma(0,0)$, $K_1(0.5,0)$, $M_1(0.5,0.5)$, $M_2(-0.5,0.5)$, $K_2(-0.5,0)$, $M_3(-0.5,-0.5)$, $M_4(0.5,-0.5)$ represent Brillouin zone symmetry points.

As can be seen in Figs. 1 and 2, air holes are situated on the corners of the square dielectric rod. Here, the α angle is defined as the rotation angle. The location and number of the air holes change the optical dispersion properties of the PC structure. The studied opto-geometrical parameters (d, α, r, and ε_r) affect absolute PBG. However, the selected parameter values can be suitable for overlapping of the TM and TE bands. So, we define an additional parameter (θ) for overlapping of the bands and obtain the greatest complete PBG (Fig. 1(b)). For this purpose, the θ angle is scanned from 0° to 90° while other parameters are constant. On the other hand, the mirror and rotational symmetries are broken; the translational symmetry is protected from being influenced. This asymmetric distortion of the symmetry of the structure allows studying the dispersion features of the designed PCs.

Figures 3(a)–3(d) demonstrate the photonic band structure for a square lattice of dielectric square rods for TE and

TM modes of PC structures whose unit cells are both depicted in Figs. 1(a)–1(d) and in the insets. The vertical axis shows dimensionless frequency values in units of c/a (c is the speed of light) and the horizontal axis shows the wave vector. The $\Gamma(0,0)$, $K_1(0.5,0)$, $M_1(0.5,0.5)$, $M_2(-0.5,0.5)$, $K_2(-0.5,0)$, $M_3(-0.5,-0.5)$, and $M_4(0.5,-0.5)$ represent the Brillouin zone as shown in Fig. 2(c). The relative width of PBG is obtained with a gap/midgap ratio of $\Delta\omega/\omega$, where ω and $\Delta\omega$ represent the center of the band gap and frequency bandwidth, respectively. The first TM band gap appears between the first and second bands for all four cases (Figs. 3(a)–3(d)). The normalized frequency range is (0.223–0.270) $\omega a/2\pi c$ with a filling fraction $f = 0.343$ for Fig. 3(a), (0.228–0.282) $\omega a/2\pi c$ with a filling fraction $f = 0.309$ for Fig. 3(b), (0.229–0.281) $\omega a/2\pi c$ with a filling fraction $f = 0.309$ for Fig. 3(c), (0.241–0.322) $\omega a/2\pi c$ with a filling fraction $f = 0.241$ for Fig. 3(d) at $d = 0.4a$. While relative widths of TM1–TM2 PBGs are 18.88%, 21.23%, 20.5%, and 29%, respectively. The observed partial TM and TE PBGs are given in Table 1. Note that the band gap region changes with unit cell shape. The largest case corresponds to Fig. 3(d). The broad band gap occurs only for the TM mode but not for the TE mode. The percentage is relatively small when we compare the two cases. The TM modes prefer an isolated configuration to support a wide band gap. On the other hand, TE modes yield a large band gap for connected lattices. The physical reasons behind this are the Maxwell boundary conditions, continuities of the tangential component of electric and magnetic fields, and continuity of the normal component of electric flux density. The broad band gaps for both TE and TM modes can be used to design high-performance polarization-insensitive, sensitive waveguides, ultra-compact switches, beam splitters, optical intensity modulators, and novel sensor topologies.

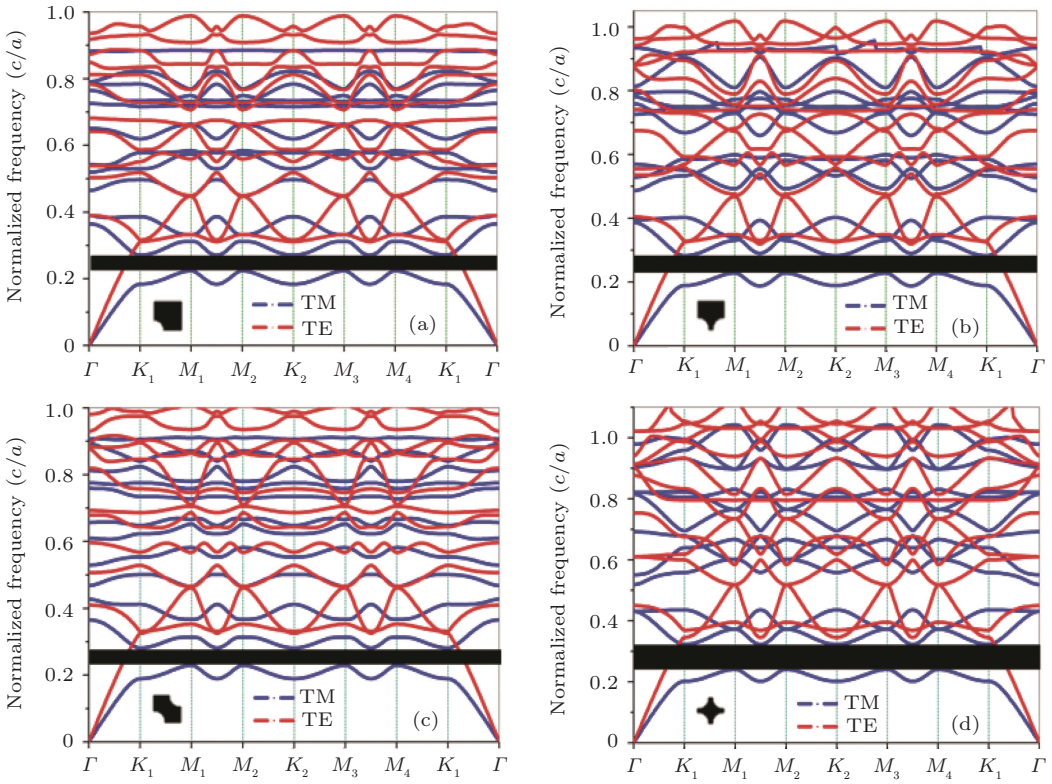


Fig. 3. (color online) TM and TE photonic band structures for a square lattice of dielectric square rods as shown in Fig. 1. The shaded region shows the absolute photonic band range between TM1 and TM2.

Band gaps for TM and TE modes appear or disappear for different rod shapes. The TM3–TM4 band gap is generally larger as shown in Table 1. The other partial TM–TE band gaps are very small except for the third structure. When figures 1(a) and 1(b) are compared with each other, it can be seen that figure 1(b) gives a wider absolute PBG, the number of observed partial band gaps decreases. Modes observed for Fig. 1(b) have mostly higher frequencies. This results from the change of the effective refractive index or in filling fraction. Adding the cylindrical air gap to a different point increases the number of observed partial PBGs as shown in Figs. 3(b) and 3(c). In this case, while the TM6–TM7 partial band gap is eliminated, TM5–TM6 and TM7–TM8 partial band gaps arise. Similar results are also observed for TE modes. The new partial PBG is due to the scattering of short wavelength light between square dielectric rods at resonance. The increase in the number of cylindrical air gaps in the corner of the square dielectric rod surprisingly expands the complete photonic band interval. For instance, the complete photonic band interval belonging to Fig. 1(d) is quite wide (29%).

Table 1. All of the other PBGs and their properties for that arrangement of PCs.

Structure	TM frequency interval (a/λ)		($\Delta\omega/\omega$)/%	TE frequency interval (a/λ)		($\Delta\omega/\omega$)/%
	TM1–TM2	0.223–0.270	18.88	TE2–TE3	0.448–0.449	0.4
	TM3–TM4	0.389–0.447	13.92	TE3–TE4	0.518–0.538	3.7
	TM4–TM5	0.497–0.520	4.46	TE4–TE5	0.576-0.586	1.75
	TM6–TM7	0.584–0.619	5.79	TE6–TE7	0.681–0.706	3.6
	TM7–TM8	0.663–0.716	7.69	TE10–TE11	0.887–0.909	2.5
	TM8–TM9	0.725–0.732	0.87	TE11–TE12	0.932–0.935	0.3
	TM11–TM12	0.822-0.881	6.9			
	TM1–TM2	0.228–0.282	21.23	TE2–TE3	0.468–0.472	0.95
	TM3–TM4	0.402–0.486	18.92	TE10–TE11	0.932–0.942	1.1
	TM6–TM7	0.599–0.659	9.62			
	TM10–TM11	0.796–0.809	1.56			
	TM11–TM12	0.905–0.913	0.86			
	TM1–TM2	0.229-0.281	20.5	TE2–TE3	0.461–0.466	0.97
	TM3–TM4	0.427–0.465	8.54	TE3–TE4	0.528–0.567	7.05
	TM4–TM5	0.501–0.529	5.40	TE4–TE5	0.596–0.641	7.22
	TM5–TM6	0.582-0.607	4.18	TE6–TE7	0.705-0.710	0.58
	TM7–TM8	0.669–0.727	8.31	TE10–TE11	0.916–0.930	1.47
	TM10–TM11	0.824-0.841	2.00	TE11–TE12	0.975–0.981	0.57
	TM11–TM12	0.893–0.905	1.25			
	TM1–TM2	0.241-0.322	29	TE4–TE5	0.666–0.667	0.27
	TM3–TM4	0.436–0.518	17.27			
	TM6–TM7	0.692–0.695	0.44			
	TM9–TM10	0.831–0.898	7.75			

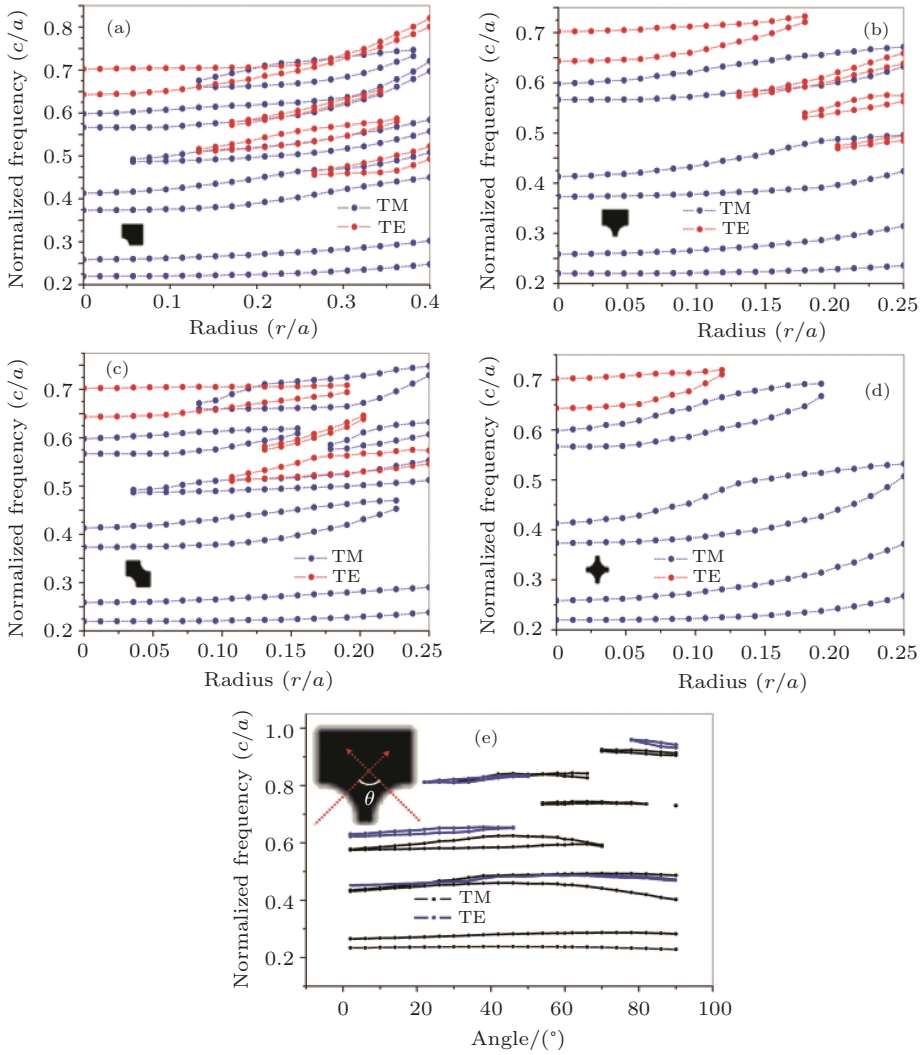


Fig. 4. (color online) Photonic gap map for the square lattice of square rods in Fig. 1.

The TM and TE gap — maps in terms of r/a ratio for all arrangements of PCs are shown in Fig. 4. The absolute PBG ($\Delta\omega$) is the difference between frequencies of upper and lower bands. The TM and TE bands overlap for some values of cylindrical air gaps, which are important criteria to design photonic crystal and polarization insensitive waveguides. In addition to these cases, the gap-map is calculated with respect to the angle ($0^\circ \leq \theta \leq 90^\circ$) between the centers of the cylindrical air gaps located in the structure in Fig. 1(b). When the angle goes from zero to 90°, the TM absolute PBG becomes wider. Hence, the improvement of the PBG can be realized with the angle between the centers of cylindrical air gaps.

Investigating unit cell modification reveals the polarization dependency of 2D PCs. Instead of starting with dielectric square rods in air background, one can use the complementary configuration square air rods in dielectric background. Then the unit cell shape will affect the TE modes more than the TM one. Lastly, the square lattice can be replaced by a hexagonal lattice. It is expected to have a larger overlap of TE and TM gaps in that case.

3. FDTD analyses of proposed photonic crystal structures

The computational analysis consists of the time-domain method based on 2D FDTD. The boundary conditions in this method are surrounded by well-matched layers to remove the back reflections coming from the ends of the finite computational window. In this regard, the Gaussian beam source in the time domain method is preferred and the beam width value is determined to be $d_f = 0.2$ in this study. For calculations, the shape of iso-frequency contours (IFCs) can be presented as an effective opinion while investigating for broad complete band ranges. At the same time, another appealing property for the worked structure can be used to design new structures with the dispersion properties of PCs. In this system, the direction of the group velocity of light is determined by the gradient of the IFCs. The original forms of dissimilar IFCs reveal the self-collimation effect together with generally following a diffraction event. Moreover, IFCs can vary according to the location of the cylindrical hole in the corner of the quadratic bar. However, the behaviors of electromagnetic waves can be determined by considering iso-frequency curves with respect to the value of the horizontal angle of the cylindrical hole. As a result, the angle parameter will generate the anisotropy situation for the second TM band. The propagation direction of the self-collimated beam can easily be arranged to guide the optical pulse throughout the PC waveguide, and so it is not visibly skewed IFC for the second band of the regular PC (Fig. 5). Besides, there are important changes such as appearances of self-collimation properties and regularities of the curves along the symmetry directions for IFCs of the designed PC structure.

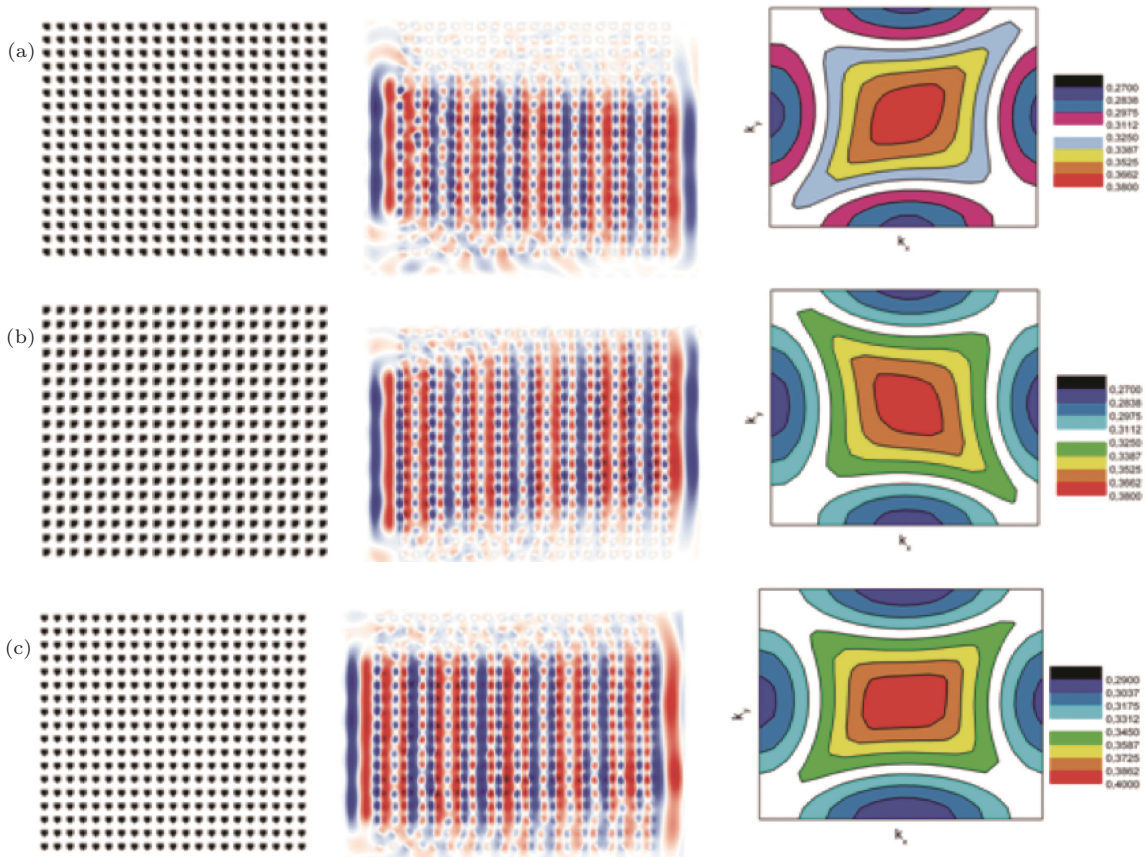


Fig. 5. (color online) Iso-frequency contours of the second TM band for structures in Fig. 1 and self-collimated light beam. The working frequency of TM mode is 0.367 $\omega a/2\pi c$ for Figs. 1(a) and 1(b). The working frequency of Fig. 1(c) is 0.372 $\omega a/2\pi c$.

It is shown in Fig. 5 that the TM modes propagate in the working PC structures in Figs. 1(a) and 1(b). While the frequencies of TM modes for Figs. 5(a) and 5(b) are approximately centered at $a/\lambda = 0.367$, the frequency of TM mode for Fig. 5(c) is almost centered at $a/\lambda = 0.372$. The difference between Figs. 5(a) and 5(b) is the position of cylindrical hole. While the horizontal angle value of it in Fig. 5(a) structure is $\alpha = -45°$, this value is $\alpha = +45°$ for Fig. 5(b). In these instances, the lattice constant a is 568.85 nm and the radius of air rod is 113.77 nm. The horizontal lengths of the three structures are all $20a$ (11.377 μm). Accordingly, the shift amount of the light is approximately equal to 1706 μm in the y direction. This value corresponds to 8.5° angularly for Figs. 5(a) and 5(b). However, for Fig. 5(c) while the horizontal angle of two cylindrical holes is $\theta = 90°$, the TM light moves along the optical axis. As a result, the light beam can be directed according to the angles and locations of air holes in the corners of dielectric rods and also the spread way of the electromagnetic wave can be determined with the IFCs.

The next calculation involves the photonic crystal structure formed with rods, which removes from the corners O_1 and O_2 (Fig. 6). For this, we combine the structure in Fig. 5(a) and that in Fig. 5(b), and so the light beam demonstrates the self-collimation effect. If we pay attention, according to the positions of the holes, the light beam is first directed downward and then upward. However, the TM mode is vigorously restricted at the sharp edges of each square dielectric rod.

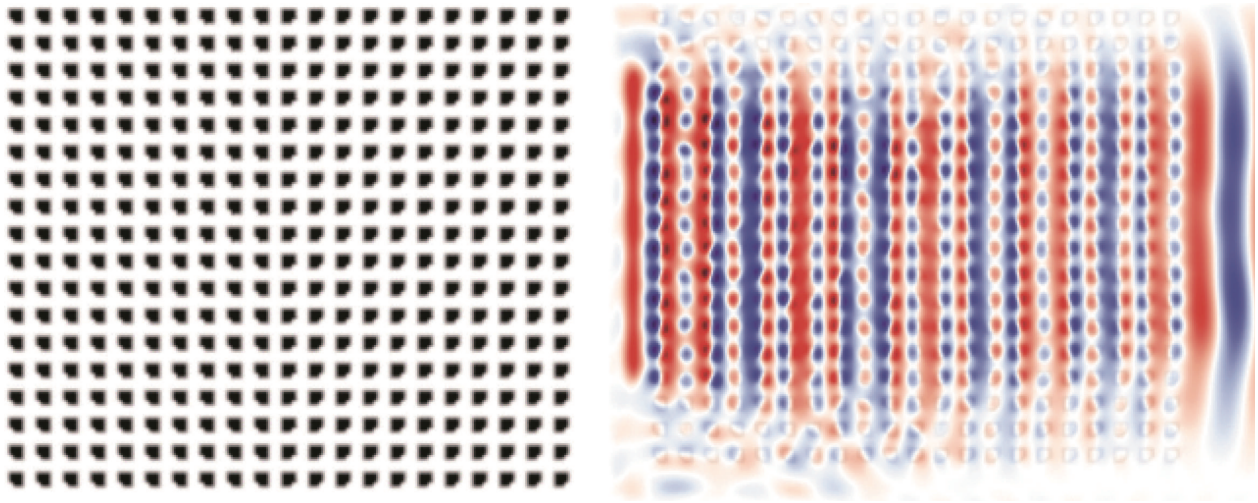


Fig. 6. (color online) Photonic crystal structure formed with rods removed from the corner O_1 and O_2. The light first propagates downward, then upward. The working frequency of the TM mode is 0.367 $\omega a/2\pi c$.

4. Photonic crystal Y branch structure

One of the important applications in optical integrated circuits in the future is planar photonic crystal waveguide technology. At the beginning of this technology, waveguide bends and Y branches come into being. The numerical and experimental researches about 2D photonic crystal waveguides include photonic crystal waveguide bends and branches show an increase.[41–45] In this context, it is believed that the proposed structure will present a new contribution to the studies of waveguide bends and Y branches. We realize the theoretical investigation for our structure and obtain the results as shown in Fig. 7. In the proposed structure, the light source is positioned on the left side of the working structure. The normalized working frequency of the TM mode is 0.376 $\omega a/2\pi c$ and the light propagates along ΓM_1 and ΓM_4. But at a certain time, it moves along a straight line (ΓK_1). Finally, the light incurs a deflection again in the directions of ΓM_1 and ΓM_4. When the normalized frequency is 0.376 $\omega a/2\pi c$, the lattice constant a is 582.8 nm and the radius of each air rod is 145.7 nm.

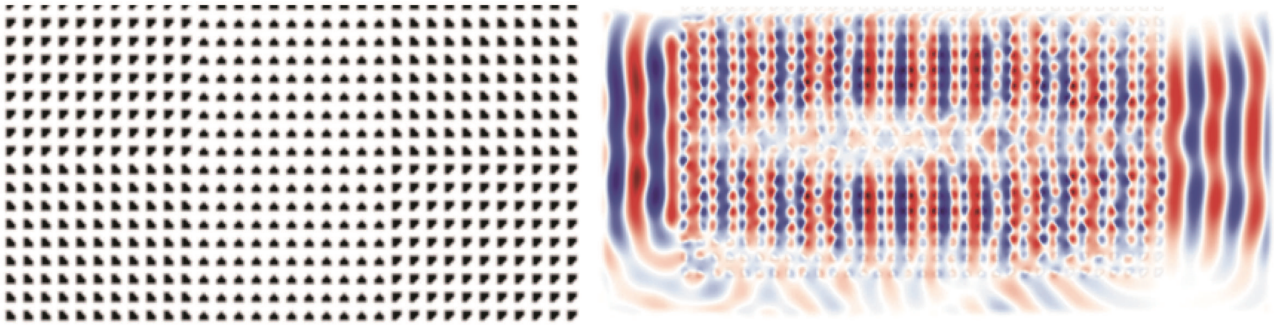


Fig. 7. (color online) Photonic crystal is Y-branch structure. Light is divided into two branches, and then spreads along a straight path.

The obtained results demonstrate that the structure, which is created by cylindrical air gaps removed from the corner of the square dielectric rod, carries anisotropic properties on the iso-frequency curves even though they are formed in an isotropic way. Moreover, light with the same polarization can move through different directions in an anisotropic medium. This shows that the structure can work as Y-junctions and a Mach–Zhender interferometer. As a result, the proposed structure reveals a situation similar to a medium with double refractive index (birefringence). Due to the limited size of the PCs, the side coupled light is usually examined. It becomes possible to light up/down directing and splitting with the proposed design. According to the research on this subject, such light manipulation scenarios are very difficult in determining the defect-type guiding mechanism, due to the fact that lattice type necessitates very sharp corners that deteriorate the transmission efficiency of light.

5. Conclusions

In this study, we demonstrate the TM and TE bands of photonic crystal structures formed by cylindrical air gaps removed from the corners of square dielectric rods in the first calculation. According to the obtained results, we show that there is a large photonic band gap between TM1–TM2 and TM3–TM4 bands. These results provide a suitable environment for the integrated optical circuit applications. In the second calculation, we realize the determination of the gap-map belonging to these structures. The obtained graphs demonstrate the effect of the radius of cylindrical air gap r and θ angle between absolute and partial photonic band gaps. Additionally, we show that TM and TE band gaps overlap at some values of the radius r and angle θ. It is thought that this overlap will ease the production of photonic crystals for the practical applications like photonic insensitive waveguide. The third calculation includes iso-frequency contours and electric field distributions. According to this calculation, the proposed structure provides a photonic crystal structure to act as beam deflecting and beam router by showing the self-collimation effect. The final calculation is about the Y-junction with a composite structure, which directs the light beam into two separate arms by the self-collimation effect. In this context, it is believed that designed structures will present a new contribution to the studies of waveguide bends and Y branches.

References

[1] Yablonovitch E 1987 *Phys. Rev. Lett.* **85** 2059
[2] Zhang L L, Liu W, Li P, Yang X and Cao X 2017 *Chin. Phys. B* **26** 064209
[3] Ba N, Wu X Y, Li D F, Wang D, Fei J Y and Wang L 2017 *Chin. Phys. B* **26** 054207
[4] Xu X W, Cui B F, Zhu Y X, Guo W L and Li W G 2012 *Acta Phys. Sin.* **61** 154213 (in Chinesey)
[5] Zong Y X, Xia J B and Wu H B 2017 *Chin. Phys. B* **26** 044208
[6] Yin Q, Xiang G Y, Li C F and Guo G C 2017 *Chin. Phys. Lett.* **34** 034207
[7] Zhou X P and Shu J 2014 *Chin. Phys. Lett.* **31** 024201
[8] Lin X S, Liu J L, Zheng Y B and Lan S 2014 *Chin. Phys. Lett.* **31** 014206
[9] Erdiven U, Tetik E and Karadag F 2017 *Optoelectron. Adv. Mater.* **11** 307
[10] Zheng Y B, Yang Y W, Jensen L, Fang L, Juluri B K, Flood A H, Weiss P S, Stoddart J F and Huang T J 2009 *Nano Lett.* **9** 819
[11] Zheng Y B, Jensen L, Yan W, Walker T R, Juluri B K, Jensen L and Huang T J 2009 *J. Phys. Chem. C* **113** 7019
[12] Zhang Q, Zhou S, Li Q H, Wang X Z and Fu S F 2012 *Acta Phys. Sin.* **61** 157501 (in Chinese)
[13] Hou J, Gao D, Wu H and Zhou Z 2009 *Opt. Commun.* **282** 3172
[14] Jia W, Jiang L, Chen K and Li X 2010 *Opt. Commun.* **283** 4078
[15] Chien H T, Chen C C and Luan P G 2006 *Opt. Commun.* **259** 873
[16] Amel L and Abdelmadjid B 2015 *Chin. Phys. Lett.* **32** 054204
[17] Kurt H, Hao R, Chen Y, Feng J, Blair J, Summers C, Citrin D S and Zhou Z 2008 *Opt. Lett.* **33** 1614
[18] Lai C F, Yu P, Wang T C, Kuo H C, Lu T C, Wang S C and Lee C K 2007 *Appl. Phys. Lett.* **91** 041101
[19] Vasic B, Isic G, Gajic R and Hingerl K 2010 *Opt. Express* **18** 20321
[20] Martínez A and Martí A J 2005 *Phys. Rev. B* **71** 235115
[21] Chien H T, Tang H T, Kuo C H, Chien C C and Ye Z 2004 *Phys. Rev. B* **70** 113101
[22] Li Z Y and Lin L L 2003 *Phys. Rev. B* **68** 245110
[23] Sesay M, Jin X and Ouyang Z 2013 *J. Opt. Soc. Am. B* **30** 2043
[24] Nguyen H M, Dundar M A, Heijden R W V D, Drift E W J M V D, Salemink H W M, Rogge S and Caro J 2010 *Opt. Express* **18** 6437
[25] Yao C X, Hui L, Shen Q Y, Fei W Y and Bo N 2008 *Chin. Phys. Lett.* **25** 4307
[26] Lu M, Juluri B K, Lin S C S, Kiraly B and Gao T 2010 *J. Appl. Phys.* **108** 103505
[27] Wu L, Li L and Zhang J 2008 *Phys. Rev. A* **78** 013838
[28] Li W S, Luo S J, Huang H M, Zhang Q and Fu Y H 2012 *Acta Phys. Sin.* **61** 164102 (in Chinese)
[29] Yan T L, Chen B, Liu G, Niu R P, Shang Jie, Gao S, Xue W H, Jin J, Yang J R and Li R W 2017 *Chin. Phys. B* **26** 067702
[30] Dong L J, Du G Q, Yang C Q and Shi Y L 2012 *Acta Phys. Sin.* **61** 164210 (in Chinese)
[31] Kurt H, Turduev M and Giden I H 2012 *Opt. Express* **20** 7184
[32] Park J M, Lee S G, Park H Y and Kim J E 2008 *Opt. Express* **16** 20354
[33] Ge C H, Li H L, Zhu X L and Pan A L 2017 *Chin. Phys. B* **26** 034208
[34] Lee S G, Oh S S, Kim J E, Park H Y and Kee C S 2005 *Appl. Phys. Lett.* **87** 181106
[35] Gao D, Zhou Z and Citrin D S 2008 *J. Opt. Soc. Am. A* **25** 791
[36] Prather D W, Shi S, Pustai D M, Sharkawy A, Chen C, Venkataraman S, Murakowski J and Schneider G 2004 *Opt. Lett.* **29** 50
[37] Jiang L Y, Wu H and Li X Y 2014 *J. Opt.* **43** 108
[38] Zhang Y, Zhang Y and Li B 2007 *Opt. Express* **15** 9287
[39] Li Y Y, Gu P F, Li M Y, Yan H and Liu X 2006 *J. Electromagn. Waves Appl.* **20** 265
[40] Wu Z, Xie K, Yang H and Jiang P 2011 *Opt. Eng.* **50** 114002
[41] Turduev M, Oner B, Giden I and Kurt H 2013 *J. Opt. Soc. Am. B* **30** 1569
[42] Wang Z Y, Yu Z H, Zheng X D and Wang L 2012 *J. Electromagn. Waves Appl.* **26** 1476
[43] Turduev M, Giden I and Kurt H 2012 *J. Opt. Soc. Am. B* **29** 1589
[44] Tayeboun F, Naoum R, Tayeboun H M, Hattori H T and Salah-Belkhodja F 2005 *J. Electromagn. Waves Appl.* **19** 615
[45] Pei T H and Huang Y T 2011 *J. Appl. Phys.* **109** 034504